Cell Tissue Res (2016) 366:1–11
DOI 10.1007/s00441-016-2413-y

REGULAR ARTICLE

Morphological and behavioral characterization of adult mice deficient for SrGAP3

Jonathan Bertram[1] · Leif Koschützke[1] · Jörg P. Pfannmöller[2] · Jennifer Esche[3] · Laura van Diepen[3] · Andreas W. Kuss[3] · Bianca Hartmann[1] · Dusan Bartsch[4] · Martin Lotze[2] · Oliver von Bohlen und Halbach[1,5]

Received: 1 March 2016 / Accepted: 14 April 2016 / Published online: 17 May 2016

Abstract SrGAP3 belongs to the family of Rho GTPase proteins. These proteins are thought to play essential roles in development and in the plasticity of the nervous system. SrGAP3-deficient mice have recently been created and approximately 10 % of these mice developed a hydrocephalus and died shortly after birth. The others survived into adulthood, but displayed neuroanatomical alteration, including increased ventricular size. We now show that SrGAP3-deficient mice display increased brain weight together with increased hippocampal volume. This increase was accompanied by an increase of the thickness of the stratum oriens of area CA1 as well as of the thickness of the molecular layer of the dentate gyrus (DG). Concerning hippocampal adult neurogenesis, we observed no significant change in the number of proliferating cells. The density of doublecortin-positive cells also did not vary between SrGAP3-deficient mice and controls. By analyzing Golgi-impregnated material, we found that, in SrGAP3-deficient mice, the morphology and number of dendritic spines was not altered in the DG. Likewise, a Sholl-analysis revealed no significant changes concerning dendritic complexity as compared to controls. Despite the distinct morphological alterations in the hippocampus, SrGAP3-deficient mice were relatively inconspicuous in their behavior, not only in the open-field, nest building but also in the Morris water-maze. However, the SrGAP3-deficient mice showed little to no interest in burying marbles; a behavior that is seen in some animal models related to autism, supporting the view that SrGAP3 plays a role in neurodevelopmental disorders.

Keywords Adult neurogenesis · Dendritic spines · Hippocampus · Golgi impregnation · MRI

Jonathan Bertram and Leif Koschützke contributed equally to this work.

✉ Oliver von Bohlen und Halbach
oliver.vonbohlen@uni-greifswald.de

[1] Institut für Anatomie und Zellbiologie, Universitätsmedizin Greifswald, Friedrich-Löffler-Straße-23c, 17487 Greifswald, Germany

[2] Funktionelle Bildgebung; Diagnostische Radiologie und Neuroradiologie, Universitätsmedizin Greifswald, Walter-Rathenau-Str. 46, 17475 Greifswald, Germany

[3] Department of Human Genetics, University Medicine Greifswald and Interfaculty Institute of Genetics and Functional Genomics, University of Greifswald, Greifswald, Germany

[4] Zentralinstitut für Seelische Gesundheit, Abt. Molekularbiologie, J 5, 68159 Mannheim, Germany

[5] Institute of Anatomy and Cell Biology, Universitätsmedizin, Friedrich Loeffler Strasse 23c, 17487 Greifswald, Germany

Introduction

Rho GTPase proteins play essential roles in the development and plasticity of the nervous system. One member of this large family is encoded by the SRGAP3 gene, which encodes the SLIT-ROBO RHO GTPase-activating protein 3 (SrGAP3), also termed mental disorder-associated GTPase-activating protein (MEGAP) or WAVE-associated GTPase-activating protein (WRP). Functional inactivation of SRGAP3 in 3p balanced translocation was observed in a patient with mental retardation (Endris et al. 2002). SrGAP3 regulates cytoskeletal reorganization through inhibition of the Rho GTPase Rac1 and interaction with actin remodeling proteins. SrGAP3 protein is highly expressed in fetal and adult brain, including the cortex and hippocampus (Endris et al. 2002; Waltereit et al. 2008). Moreover, the highest *SrGAP3* mRNA expression in the adult mouse brain can be found in the hippocampus, in the pyramidal layers of areas CA1–CA3 and in the granular layer

of the dentate gyrus (http://mouse.brain-map.org/experiment/show/316).

To investigate the possibility that disruption of the SRGAP3 gene causes anatomical and behavioral defects, SrGAP3-deficient mice have been generated. Currently, two different SrGAP3 models are available; a conditional SrGAP3 knockout mouse (Carlson et al. 2011; Kim et al. 2012), in which SrGAP3 is deleted in nestin-positive cells, and a SrGAP3-deficient mouse that mimics the disruption of SrGAP3 reported in a patient with severe intellectual disability (Waltereit et al. 2012). There are certain differences in the phenotype of these mice. Thus, for the conditional SrGAP3 knockout mice, reductions in hippocampal spine densities have been reported (Carlson et al. 2011), whereas in SrGAP3-deficient mice the hippocampal spine densities are not greatly affected, but the morphology of individual hippocampal dendritic spines is (Waltereit et al. 2012). Concerning the conditional SrGAP3 knockout mice, no differences were found by comparing these mice with their controls in the open field, but significant impairments were seen in behavioral tests such as novel object recognition, water maze, and passive avoidance (Carlson et al. 2011). In contrast to this, male SrGAP3-deficient mice have been reported to be less active than wild-type mice in the open field test, express lower locomotor activity, and display tics and impairments in spontaneous alternation (Waltereit et al. 2012).

It has been described that conditional SrGAP3-deficient mice display severe disturbances in adult neurogenesis, with abnormal progenitor migration affecting the subventricular zone (SVZ) and rostral migratory stream (Kim et al. 2012). Moreover, it has been shown in vitro that lentivirus-mediated knockdown of SrGAP3 dramatically decreases viability and proliferation of cortical immature neural stem cells/neural progenitor cells (Lu et al. 2013). Aside from the SVZ, the dentate gyrus (DG) is also capable of adult neurogenesis. Neurogenesis within the DG occurs throughout postnatal life, but in contrast to neurogenesis in the SVZ, is influenced by the environment, behavior, and learning as well as aging (Dokter and von Bohlen und Halbach 2012; Kempermann 2012; Marlatt et al. 2012).

Based on these data, we hypothesized that mice deficient for SrGAP3 display alterations in the morphology and function of the hippocampus. Therefore, we examined the gross morphology of the hippocampal formation of adult SrGAP3-deficient mice. Since we noted an increase in the size of the hippocampus, we analyzed this brain region in more detail (adult neurogenesis within the DG, densities and size of dendritic spines in the DG and dendritic complexity of adult granule cells in the DG). Furthermore, we analyzed the SrGAP3-deficient mice concerning their behavior in tests that are related to the hippocampal formation.

Materials and methods

SrGAP3-deficient mice (Waltereit et al. 2012) and their controls were obtained from crosses of heterozygous SrGAP3-deficient mice. For experiments, 3- to 4-month-old male homozygous SrGAP3-deficient mice and their controls ($SrGAP3^{+/+}$) were used. All animal procedures were performed in accordance with the European Communities Council Directive of 1986 and the institutional guidelines for animal welfare.

Post-mortem magnetic resonance imaging (MRI)

Post-mortem MRI was performed as recently described in detail by von Bohlen und Halbach et al. (2014). In brief: adult mice were euthanized and transferred to a 7 Tesla ClinScan animal scanner (BioSpin; Bruker, Ettlingen, Germany) with a bore of 15.4 cm. A 2 × 2 channel mouse headcoil was used to measure a 3D T2-weighted turbo-spin echo (TSE) sequence [96 transversal slices, 100 μm thickness, no gap, matrix of 1024 × 1024 pixels, repetition time (TR) = 2500 ms, echotime (TE) = 55 ms]. The scanning was optimized to achieve about 95 images, covering the whole brain of the mouse and adjacent tissue, with a resolution of $x = 0.025$; $y = 0.025$, $z = 0.1$ millimeters per pixel. For reconstruction and visualization of the data Neurolucida (MBF Biosciences, USA) was used.

Histology

Animals were euthanized with diethyl ether and transcardially perfused with phosphate-buffered saline (PBS) and afterwards with 4 % paraformaldehyde (PFA). Thereafter, brains were removed and wet weight was determined using an analytical balance (Acculab, Germany). To ensure a complete fixation, the whole brains were stored in 4 % PFA for 3 days.

DAPI staining Serial coronal sections (30 μm) were cut using a vibratome (VT1000S; Leica, Germany), collected and stored in 20 % ethanol. Sections were mounted on SuperFrost® Plus slides. Sections were incubated for 5 min in a PBS-solution containing DAPI (4′,6-diamidino-2-phenylindole; 1:10,000). Sections were mounted in fluorescent mounting medium (Dako, Carpinteria, CA, USA). Regions of interest from one focal plane were captured by an AxioCam camera mounted on an Axioplan 2 imaging microscope under the control of Axiovision 3.1 software (all from Zeiss, Germany). The mean thickness was analyzed using ImageJ (NIH, USA). The mean thickness of the granular layer was determined as the mean thickness of the granular band in which the cell nuclei were visualized with DAPI. The molecular layer was defined as the layer between the granular layer and the hippocampal fissure. Per animal, six different sections were chosen and in each section three different ROIs were analyzed.

Immunohistochemistry Sections (30 μm) were cut using a vibratome (Leica VT1000; Germany) stored in 20 % ethanol and then incubated for 30 min in a solution with 0.4 % Triton X-100 in PBS, followed by an incubation for 1 h in a solution containing 0.3 % Triton X-100 and 3 % BSA (bovine serum albumin) in PBS. For phosphohistone-H3 immunohistochemistry, sections were first mounted on SuperFrost® Plus slides. Antigen-demasking was performed for 20 min in 10 mM sodium-citrate-buffer (pH 6.0) in a microwave at 700 W. Afterwards, sections were incubated in a PBS-solution containing 5 % normal goat serum (NGS), 5 % BSA and 0.1 % Triton for 1 h. Sections were incubated in a solution containing α-phosphohistone H3 antibodies (rabbit polyclonal anti-phosphohistone H3 (sc-8656-R; Santa Cruz Biotechnology, USA) 1:100 in PBS containing 5 % BSA and 0.1 % Triton) for 2 h. Visualization of the primary antibodies was performed using Cy3-conjugated goat anti-rabbit IgG (Jackson ImmunoResearch, Germany; 1:2000 in PBS containing 5 % BSA and 0.1 % Triton-X-100 for 1 h). For doublecortin (DCX) immunohistochemistry, sections were incubated free-floating in a solution containing antibodies directed against doublecortin (goat polyclonal α-doublecortin (sc-8066; Santa Cruz Biotechnology) 1:100 in PBS containing 0.1 Triton X-100 and 3 % BSA in PBS) overnight. Thereafter sections were rinsed in a solution containing 0.3 % Triton X-100 and 3 % BSA. For visualization of the primary antibodies, Cy3-conjugated goat anti-rabbit IgG (Jackson ImmunoResearch; 1:2000 in PBS for 2 h) were used. After visualization of the primary antibodies, the sections were rinsed. For visualization of cell nuclei, sections were incubated for 5 min in a PBS-solution containing DAPI (1:10,000). After a final step of rinsing, sections were embedded in MOWIOL (Calbiochem, Germany). All slices were examined using an Axioplan 2 imaging microscope fitted for fluorescence and equipped with a digital camera. Cell counts throughout the dentate gyrus were performed directly on screen.

Golgi-Impregnation (dendritic spine analysis and Sholl-analysis) Whole brains were impregnated according to the Golgi-Cox procedure using FD Rapid GolgiStain™ Kit (FD NeuroTechnologies, USA) and cut at 120 μm. Sections were mounted on gelatinized glass slides, dehydrated, rinsed in Xylol and finally embedded in Merckoglas® (Merck Millipore, Germany). Analysis of dendritic spines was conducted blind to the experimental conditions. Only dendrites were evaluated, which displayed no breaks in their staining and which were not obscured by other neurons or artifacts (von Bohlen und Halbach et al. 2006). Since dendritic spines differ in their morphology, spines were classified into different categories (filopodia, stubby, thin, and mushroom) and their frequency was analyzed. Quantitative three-dimensional analyses of dendritic fragments with their spines were conducted using a combined hardware/software system (NeuroLucida) controlling the *x*–*y*–*z* axis (step size in *z*-axis: 0.25 μm) of the Axioplan Imaging microscope and a microscope-mounted digital camera. The three-dimensional reconstruction was done using a ×100 objective (NA: 1.4; oil immersion). Spine densities and mean spine length were calculated from the reconstructed dendrites with the help of NeuroExplorer (MBF, USA). For each brain, about 40 different neurons were sampled. For reconstruction of complete Golgi-impregnated neurons, *z*-stacks (step-width 1 μm) were generated using a high-resolution digital camera (AxioCam) attached to a microscope with a motorized stage (Axioplan Imaging), controlled by the custom-made software AxioVision (Zeiss, Germany). Neurons were imaged at low magnification and *z*-stacks were generated. These *z*-stacks were used for Sholl analysis (Sholl 1953). The Sholl analysis was obtained using Neurolucida software, which calculates the cumulative number of dendritic intersections at 25-μm-interval distance points from each neuron starting from the cell body. The number of nodes and of intersections was calculated as an index for total dendritic complexity. For that analysis, brains of six control and five SrGAP3-deficient mice were used and for each brain about 14 different neurons were sampled.

Behavioral analyses

Open field For open field tests, a quadratic 60 × 60 cm arena was used (Panlab, Spain). Illumination was set to 25 lux. Animals (controls: $n = 8$; SrGAP$^{-/-}$: $n = 14$) were placed in the middle of the area and allowed to explore for 5 min. Movements were recorded by a webcam. Parameters characterizing open-field behavior (total distance moved, velocity, resting time, centre time and defecation) were analyzed from recorded sessions using SmartJunior 1.0.0.7 (Panlab). Ethanol 70 % was applied for intertrial cleaning.

Novel object recognition For this test, a quadratic 60 × 60 cm arena was used (Panlab, Spain). Illumination was set to 25 lux. We used a standard protocol for novel object recognition (Puma and Bizot 1998). In brief: two objects were placed in the open field arena. The mouse was allowed to explore the items for 5 min. The mouse was removed and one object was randomly displaced by another object. The mouse was placed again in the open field arena for 2 min. The mouse was monitored and the behavior was analyzed using SmartJunior 1.0.0.7 (Panlab). Ethanol 70 % was applied for intertrial cleaning. For this test, nine SrGAP3-deficient mice as well as nine control mice were used.

Hole-board test The hole-board was an elevated platform (40 × 40 cm), containing 16 holes equipped with IR break beam sensors. Illumination was set to 25 lux. After animals (controls: $n = 8$; SrGAP$^{-/-}$: $n = 13$) were transferred to the platform, they were allowed to explore for 5 min. The number of

head dips was recorded using the LE8825 data logger and SedaCom v.2.0 (Panlab). Ethanol 70 % was used for intertrial cleaning. In this configuration, the apparatus is used to analyze exploratory behaviors (Sharma et al. 2010).

Dark/light box The dark/light box was divided into a 30 × 30 cm bright compartment (350 lux) and a 20 × 30 cm dark compartment. Mice (controls: $n = 8$; SrGAP$^{-/-}$: $n = 14$) were placed in the bright compartment and tracked over 5 min using a video-camera. The dark/light box is a common test for measuring anxiety-like behavior (Powell et al. 2004).

Nest building Non-maternal nest building performance has been shown to be sensitive to hippocampus damage (Jirkof 2014) and is sensitive for anxiolytic agents (Li et al. 2006). Nest building was analyzed using a standard protocol (Deacon 2006a). In brief: in the evening, nest building material (3 g each) were placed in the "home" cage of single mice with wood-embedding without any environmental enrichment items. The next morning, the nests were assessed on a rating scale of 1–5 (1: nestlets nearly untouched; 2: nestlets partially torn; 3: nestlets mostly shredded but no identifiable nest; 4: identifiable but flat nest; 5: near perfect nests). For this test, six SrGAP3-deficient mice as well as 6 control mice were used.

Morris water maze The Morris water maze provides a comprehensive assay of spatial reference memory (Vogt et al. 2008; von Bohlen und Halbach et al. 2006). The animals were expected to find a platform (14 × 14 cm^2, Plexiglas) 2 cm underneath the surface within a water-filled circular pool (diameter: 140 cm) with the help of visual cues attached at the surrounding walls. The water was rendered opaque with 2 l milk, kept at 23 ± 1 °C and renewed daily. Lighting was set to 25 lux. Animals (controls: $n = 8$; SrGAP$^{-/-}$: $n = 8$) were trained for 4 days with a total of 24 trials (6 trials per day, inter-trial interval ~1 h) during which the position of the platform was kept unchanged (acquisition phase). In each swim trial during the acquisition phase, mice were left in the pool for a maximum of 120 s or until they found the platform. On the fifth day, the platform was removed and the mouse was swimming for 60 s (probe trial) to assess memory. With a video camera suspended above the center of the pool, the swim tracks of the mice were recorded and analyzed using SmartJunior 1.0.0.7 (Panlab). The following variables from the recorded paths were analyzed: time to find platform (s), length of swim path (m), velocity (cm/s), percentage of time spent moving, percentage of time spent within a rim of 22 cm from the wall (thigmotaxis), and percentage of time swimming parallel to the wall. Additional parameters in the probe trial were percentage of time in target and other quadrants as well as the number of crossings over the former platform position.

Marble burying The marble burying test is used as a test, e.g., for obsessive–compulsive disorder (Li et al. 2006) and is sensitive to hippocampal malfunctions (Bahi and Dreyer 2012). To test marble burying, the protocol introduced by Deacon (2006b) was used. In brief, cages were filled approximately 5 cm deep with wood chip bedding, lightly tamped down to a flat, even surface. A regular pattern of glass marbles was placed on the surface, evenly spaced, each about 4 cm apart. The animal was placed in the cage for 30 min. Thereafter, the number of marbles buried (to 2/3 their depth) with bedding were counted.

Statistics

For statistical evaluation, the software PRISM 6.01 (GraphPad, USA) was used. Datasets were statistically compared either using one-way ANOVA followed by a Bonferroni's multiple comparisons test or unpaired *t* test. For the analysis of marble burying, a non-parametric Mann-Whitney *U* test was used. A p value of less than 0.05 was considered as significant. Data are expressed as mean ± SEM, except for Fig. 5b (as indicated in the legend).

Results

Brain weight and hippocampal volume are increased in adult SrGAP3-deficient mice

SrGAP3-deficient mice that did not die from hydrocephalus shortly after birth display an enlargement of the ventricles (Koschützke et al. 2015; Waltereit et al. 2012) and an increased volume of brain matter (Koschützke et al. 2015). Interestingly, the wet weight of the brains of SrGAP3-deficient mice was significantly increased by ~20 % (SrGAP3$^{-/-}$ ($n = 11$): 0.56 ± 0.004 g; control ($n = 11$): 0.45 ± 0.022 g; $p \leq 0.001$; Fig. 1a). Next, we analyzed the hippocampal volume by reconstruction of post-mortem MRI and could show that the hippocampal volume of the SrGAP3-deficient mice was significantly increased as compared to controls (SrGAP3$^{-/-}$ ($n = 4$): 27.9 ± 0.94 mm^3; controls ($n = 4$): 25.0 ± 0.57 mm^3; $p = 0.037$; Fig. 1b, c).

Adult SrGAP3 deficient mice display an enlargement of the dentate gyrus (DG)

We next analyzed whether morphological changes in the DG or area CA1 may contribute to the increase in hippocampal volume seen in the SrGAP3-deficient mice. In detail, we analyzed the thicknesses of different layers (granular and

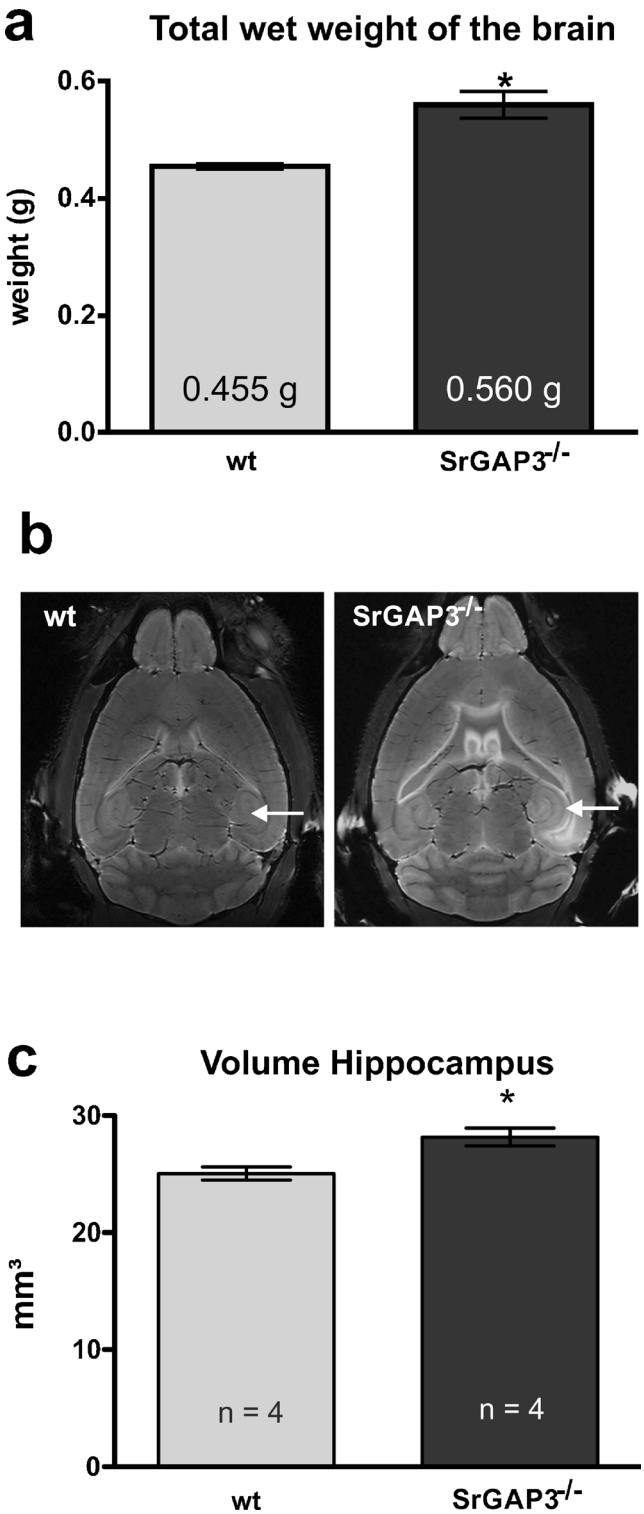

Fig. 1 Gross morphology of the brains of SrGAP3$^{-/-}$ mice. The total weight of the brains of SrGAP3 deficient mice was found to be increased (**a**). Moreover, MRT scans show that the brains of SrGAP3 deficient mice display enlarged ventricles as compared to their controls (**b**). A detailed analysis of the hippocampal formation revealed that the total hippocampal volume (the hippocampus is marked by an *arrow* in (**b**)) was increased in the case of SrGAP3-deficient mice (**c**)

molecular layer) of the DG as well as of area CA1 (pyramidal layer and the *stratum oriens*) on serial sections.

The mean thickness of the granular layer of the DG (Fig. 2a, c, d) was not significantly altered (+4.6 %) in SrGAP3-deficient mice (90.85 ± 3.95 μm; $n = 4$) as compared to their age-matched controls (86.86 ± 3.29 μm; $n = 4$). The mean thickness of the molecular layer (Fig. 2b–d), however, was significantly increased (+13.8 %; $p = 0.0046$) in SrGAP3-deficient mice (233.2 ± 3.65 μm; $n = 4$) as compared to their age-matched controls (204.9 ± 5.28 μm; $n = 4$).

Comparable to these results, we found that the thickness of pyramidal layer of area CA1 was not significantly affected in SrGAP3-deficient mice (+3.3 %; Fig. 2e), but the thickness of the *stratum oriens* of area CA1 was affected (Fig. 2f). Within SrGAP3-deficient mice, the thickness of the *stratum oriens* was strongly increased by 24.5 % as compared to controls (SrGAP3$^{-/-}$: 208.5 ± 6.93 mm; control: 167.5 ± 3.81 mm; $p = 0.002$).

Adult hippocampal neurogenesis is unaffected in adult SrGAP3 deficient^{-} mice

We next investigated whether SrGAP3-deficient mice display changes in adult hippocampal neurogenesis. We first analyzed whether altered proliferation within the DG can be noted. For that purpose, we used the marker phosphohistone H3 (pH3). The marker is specific for dividing cells, regardless of whether these cells are neuronal or non-neuronal (von Bohlen und Halbach 2011). SrGAP3-deficient mice displayed no statistical significant alteration in the number of pH3-positive cells within the DG ($p = 0.094$; Fig. 3a, b).

Doublecortin (DCX) is a marker for the neuronal lineage. DCX is expressed in the adult DG in late mitotic active neuronal cells, as well as in young, postmitotic neuronal cells (Couillard-Despres et al. 2005). Analysis of the population of DCX-positive cells within the DG did not reveal a significant difference between the analyzed groups (SrGAP3$^{-/-}$: 5569 ± 456 DCX-positive cells; controls: 5540 ± 679 DCX positive cells; $p = 0.974$; Fig. 3).

No difference in the morphology of adult granule cells in the DG of SrGAP3 deficient mice and corresponding controls

It has previously been described that SrGAP3-deficient mice (Waltereit et al. 2012), as well as conditional SrGAP3 knockout mice (Carlson et al. 2011), display altered dendritic spines in cortical layers, as well as in hippocampal CA regions (Carlson et al. 2011; Waltereit et al. 2012). Therefore, we investigated the density and

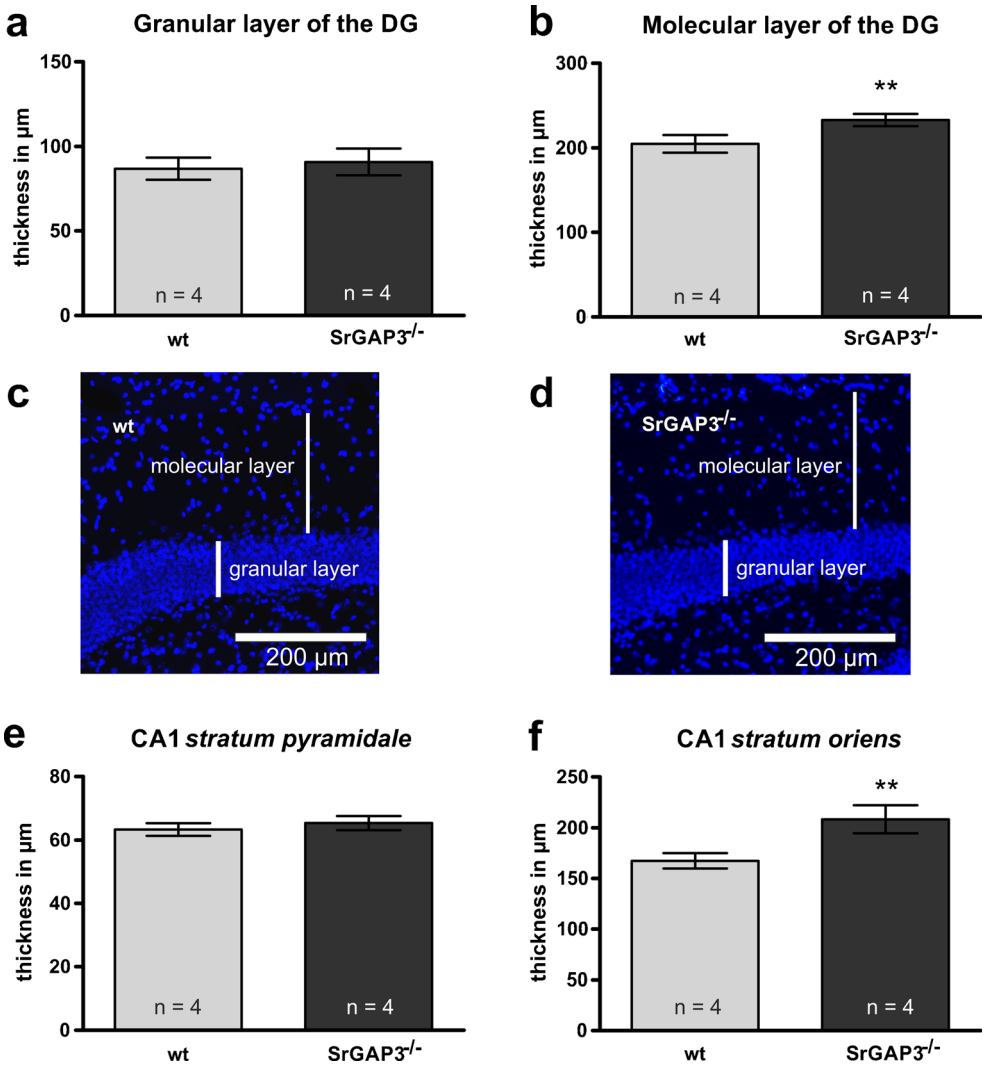

Fig 2 Analysis of the mean thickness of different hippocampal layers. The mean thicknesses of the granular layer (**a**) and molecular layer (**b**) of the DG were analyzed using DAPI-stained coronal sections. Whereas the granular layer was not significantly affected (**a**), a significant increase in the thickness of the molecular layer (**b**) by 13.8 % was noted in the SrGAP3-deficient mice (*ko*) as compared to their age-matched controls (*wt*). Examples of DAPI stained sections including the granular and molecular layer of the DG are shown for control (*wt*) mice (**c**) as well as for srGAP3 knockout mice (**d**). Analysis of the thicknesses of the *stratum pyramidale* and *stratum oriens* of area CA1 revealed that in SrGAP3-deficient mice the thickness of the *stratum pyramidale* (**e**) was unaltered, but that the mean thickness of the *stratum oriens* (**f**) was significantly increased

length of dendritic spines within the adult DG by three-dimensional reconstructions of Golgi-impregnated dendrites and computer-assisted analysis in SrGAP3-deficient ($n=6$) and control mice ($n=5$). The analysis revealed that deficiency for SrGAP3 neither affects spine densities ($p=0.772$) nor spine length ($p=0.944$; Fig. 4a–c). Moreover, no difference in the frequency of different dendritic spine categories (filopodia, stubby, thin and mushroom spines) was found by comparing SrGAP3-deficient and control mice (data not shown).

In order to investigate whether the dendritic complexity of the adult granule cells might be affected, a Sholl-analysis was performed. The statistical analysis by one-way ANOVA revealed overall differences in the distribution pattern concerning the nodes ($F_{17,89}=39{,}04$; $p\leq0.0001$) and intersections ($F_{17,89}=24{,}1$; $p\leq0.0001$). However, a subsequent post-hoc analysis (Bonferroni's multiple comparisons test) revealed no significant differences by comparing the two groups directly (Fig. 4d–f).

SrGAP3$^{-/-}$ mice show relatively normal behavior, but they failed to solve the marble burying task

First, normal behavior was monitored using the open field test. The SrGAP3-deficient mice did not display altered behavior in the open field test (total distance travelled (Fig. 5a), velocity, resting time, center time or defecation (data not shown)). Likewise, SrGAP3-deficient mice did not display altered novel object behavior (time to approach the novel object: SrGAP3$^{-/-}$: 0.45 ± 0.45 s; control: 1.00 ± 0.88; $p=0.58$).

In the hole-board test, SrGAP3-deficient mice did not differ in their behavior from their controls. Thus, the number of head dips was not different (SrGAP3$^{-/-}$: 22.1 ± 2.9 head dips; control: 25.6 ± 6.5 head dips; $p=0.586$). Likewise, the distance travelled and the velocity of the animals was not different (data not shown).

In the dark-light box, the SrGAP3 knockout mice also did not differ from controls. They travelled nearly the same distance during the test (SrGAP3$^{-/-}$: 1839 ± 128.9 mm; control:

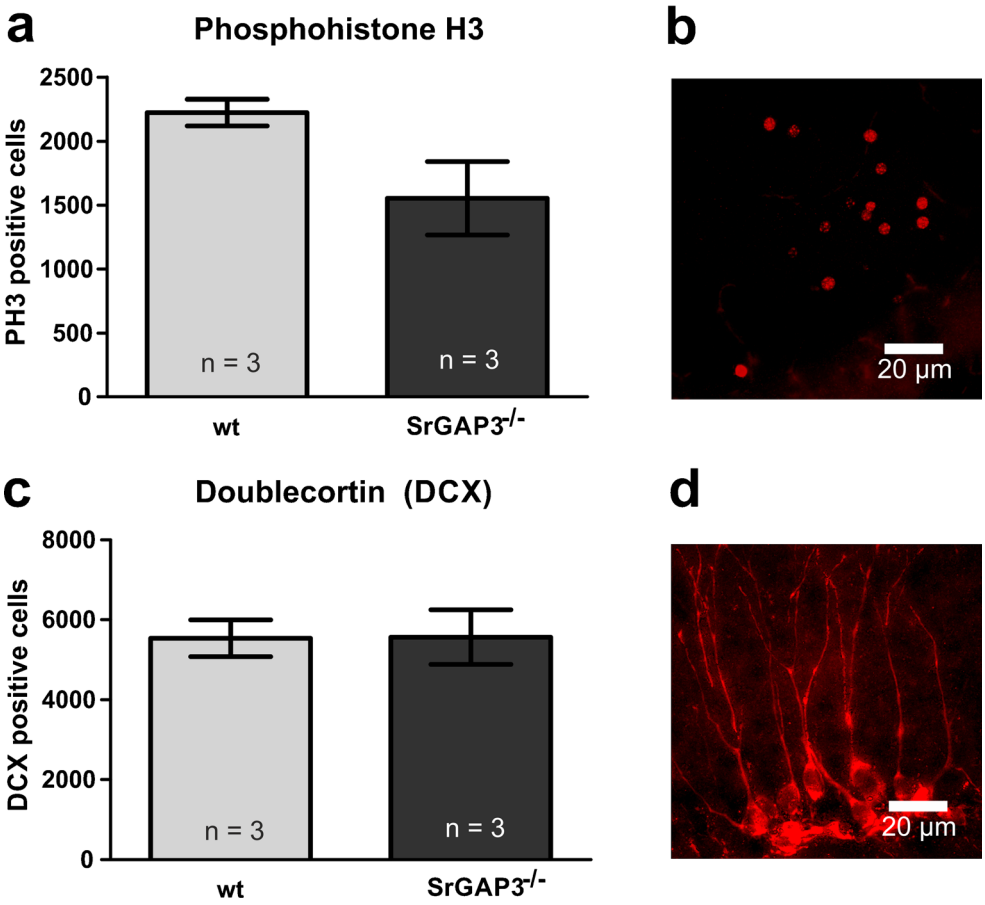

Fig 3 Analysis of adult neurogenesis in the dentate gyrus. Adult SrGAP3-deficient mice (*ko*) have nearly the same numbers of phosphohistone H3-positive cells within the adult DG (**a**), as compared to age-matched control mice (*wt*). An example of phosphohistone H3 positive cells in the DG are shown in (**b**). Analysis of the numbers of doublecortin (DCX)-positive cells in the DG of age-matched-control (*wt*) and SrGAP3-deficient mice (*ko*) revealed no significant alteration (**c**). An example of DCX positive neurons in the DG is shown in (**d**)

2200 ± 190.7 mm; $p = 0.121$) and they display the same number of entries into the light compartment (SrGAP3$^{-/-}$: 2.88 ± 0.83; control 3.11 ± 1.45; $p = 0.88$).

Since the non-maternal nest building performance has been shown to be sensitive to hippocampal changes (Jirkof 2014), we next examined the mice with respect to their nest building behavior. Again, no behavioral alteration was found ($p = 0.87$; Fig. 5b). A further behavior that is related to the hippocampal formation is the Morris water maze test. The analysis indicate that both SrGAP3$^{+/+}$ as well as SrGAP3$^{-/-}$ mice learned the Morris water maze task (Fig. 5c). The two groups of mice did not differ in their behavior in the probe trail of the test (Fig. 5d).

Despite the fact that in most behavioral tasks SrGAP3-deficient mice did not show altered behavior, it is known that SrGAP3$^{-/-}$ mice have impaired social behavior (Waltereit et al. 2012). This behavior may be homologous to endophenotypes of autism spectrum disorder. Some mouse models of autism spectrum disorder have been shown to display specific failures in the marble burying test (Egashira et al. 2007; Kouser et al. 2013). In addition, this test is sensitive to hippocampal malfunctions (Bahi and Dreyer 2012). We therefore analyzed the mice in the marble burying task. We could demonstrate a specific failure of SrGAP3$^{-/-}$ mice in this task ($p = 0.005$; Fig. 5e). Whereas controls buried about 10 marbles (control: 9.88 ± 1.8 marbles per time), the SrGAP3-deficient mice only buried 2 marbles (SrGAP3$^{-/-}$: 2.00 ± 1.5 marbles per time).

Discussion

It has been shown that SrGAP3 is highly expressed in the adult murine hippocampal formation, including the DG (Endris et al. 2002; Waltereit et al. 2008). We have previously shown that deficiency for SrGAP3 affects the hippocampal CA1 area (Waltereit et al. 2012). Based on the strong expression of SrGAP3 in the adult DG, we evaluated whether granule cells are affected in a comparable manner. Moreover, since the DG is capable of functional adult neurogenesis, we further analyzed whether SrGAP3 may have an impact upon adult neurogenesis. A first analysis of the gross morphology of the DG revealed that the thickness of the granule layer was not significantly altered in SrGAP3-deficient mice, indicating that no major cell loss occurred in this area. However, it might be possible that adult neurogenesis within the hippocampus is affected in these mice, since it has been shown that knockdown of SrGAP3 down-regulates the number of cortical

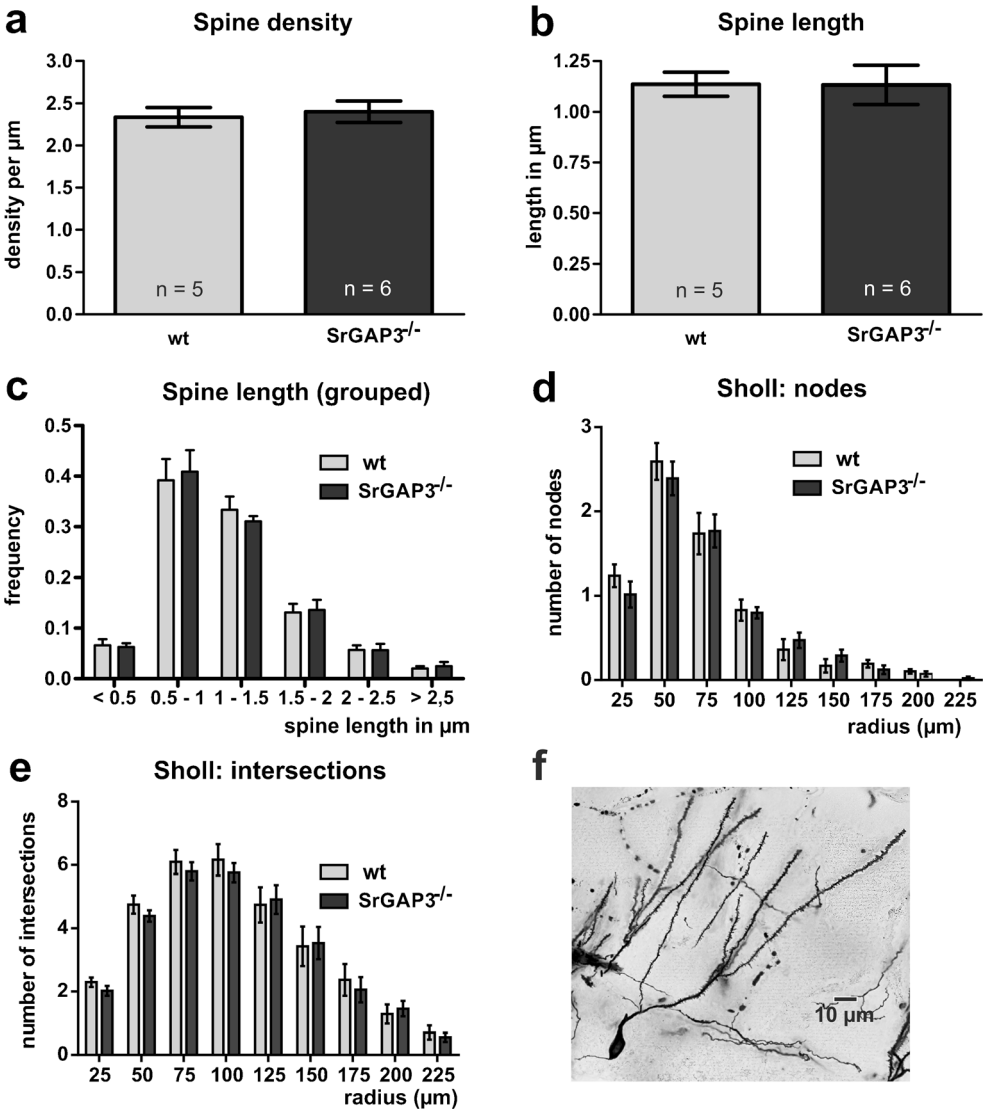

Fig. 4 Analysis of Golgi-impregnated material. Golgi-impregnated dendrites were three-dimensionally reconstructed and analyzed. There was no statistical difference by comparing dendrites of age-matched adult control (*wt*) and SrGAP3 deficient mice (*ko*) concerning spine densities (**a** wt: $n = 5$; ko: $n = 6$) or length of dendritic spines [**b** mean spine length; **c** frequency of spines, grouped for length; (wt: $n = 5$; ko: $n = 6$)]. Sholl analysis, performed on Golgi-impregnated neurons within the dentate gyrus of adult control (*wt*) and SrGAP3-deficient mice (*ko*), revealed no obvious differences in the branching pattern of the neurons, as, e.g., in the number of nodes (**d**) and intersections (**e**). An example of Golgi-impregnated neurons within the DG is displayed in (**f**)

neuronal stem cells, derived from embryonic rats (E14) in vitro (Lu et al. 2013). Furthermore, conditional SrGAP3 knockout mice were previously shown to display mislocated DCX positive cells in the corpus callosum that are thought to stem from the subventricular zone (Kim et al. 2012). Moreover, in a mouse model of mental retardation [FMRP knockout; functional loss of FMRP results in an intellectual disability (fragile X syndrom (FXS)], reduced adult hippocampal neurogenesis has been described (Guo et al. 2011). However, we did not find major alterations in adult hippocampal neurogenesis in SrGAP3-deficient mice.

SrGAP3 also dynamically regulates the cytoskeletal reorganization through inhibition of the Rho GTPase Rac1 and interaction with actin remodeling proteins. SrGAP3-mediated reorganization of the actin cytoskeleton is crucial for the normal development of dendritic spines, and loss of SrGAP3 leads to abnormal synaptic activity (Bacon et al. 2013). Conditional SrGAP3 knockout mice display a loss of dendritic spines on CA1 pyramidal neurons (Carlson et al. 2011), whereas SrGAP3-deficient mice did not show a significant loss of spines in area CA1, but a change in the morphology of dendritic spines within area CA1 (Waltereit et al. 2012). However, in contrast to pyramidal neurons, neither spine densities nor the mean length of dendritic spines were altered in the granule cells of the DG. In addition, we did not observe a reduction in the number of mushroom spines in the DG of SrGAP3-deficient mice, as has been observed in area CA1 of conditional SrGAP3 knockout mice (Carlson et al. 2011). Since SrGAP3 is known to regulate cytoskeletal reorganization, we further examined the morphology of the adult granule cells in the DG. However, we did not find evidence for altered dendritic complexity, indicating that gross morphological alterations in the granule cells of the DG are absent. SrGAP3 is strongly expressed in the adult DG, but, based on these results,

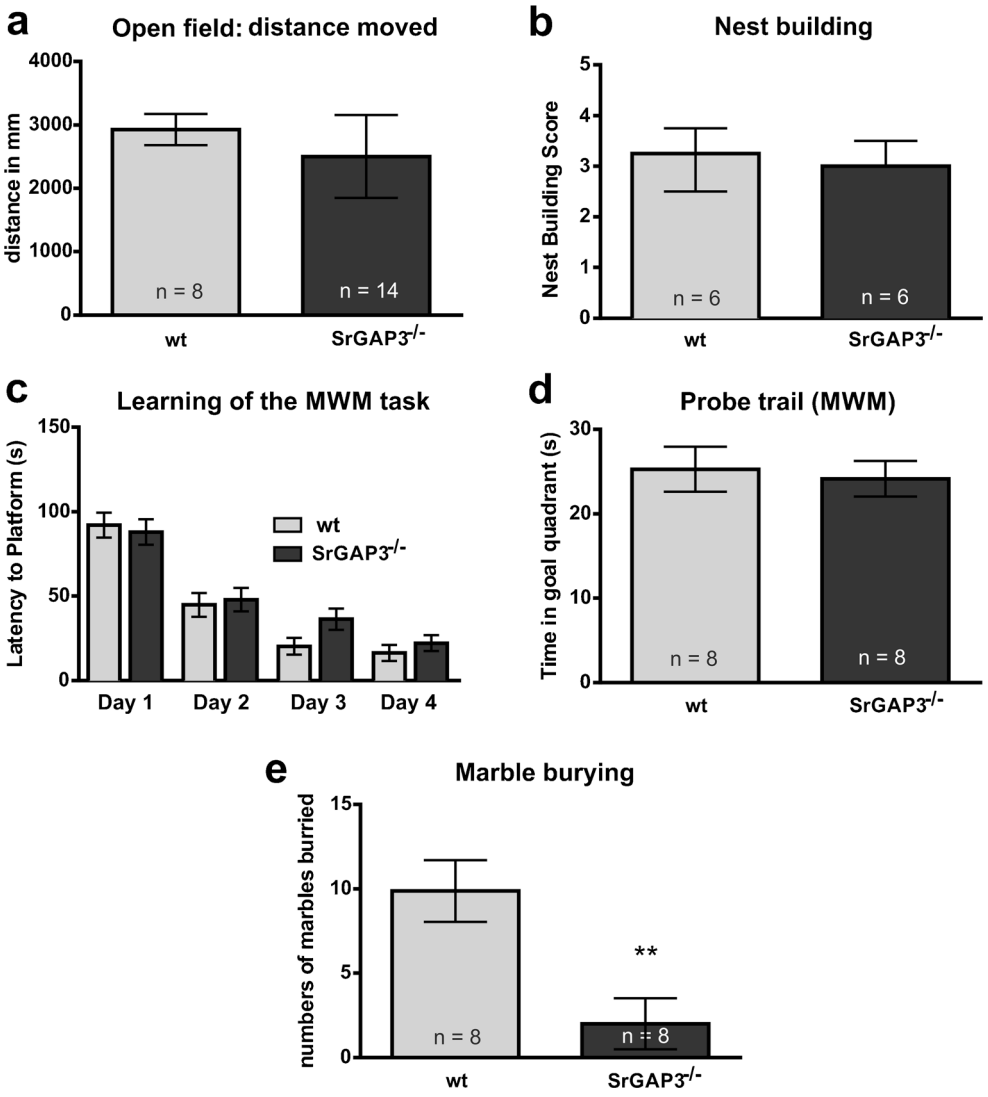

Fig. 5 Behavioral analysis of SrGAP3$^{-/-}$ mice. The SrGAP3$^{-/-}$ mice did not differ in their behavior from age-matched controls in the open field test, as, e.g., in the total distances travelled (**a**). Despite changes in the morphology of the hippocampal formation, the SrGAP3$^{-/-}$ mice did not differ in their nest building behavior (**b**; data are displayed as median with interquartile range, as described by Deacon (2006a)). Both SrGAP3$^{+/+}$ and SrGAP3$^{-/-}$ mice did not differ in their behavior in learning the Morris water maze (MWM) task (**c**). Likewise, in the probe trail of the MWM test, the SrGAP3$^{-/-}$ mice did not differ in their behavior as compared to SrGAP3$^{+/+}$ mice (**d**). However, in contrast to SrGAP3$^{+/+}$ mice, the SrGAP3-deficient mice failed to solve the marble burying task (**e**)

the role of the protein in this brain area remains enigmatic. A gene expression analysis by RNA sequencing of the whole brain hinted towards differentially expressed genes (not shown). However, a detailed gene expression analysis of the DG or hippocampus may be more helpful, as differences in gene expression could be indicative of changes on a subcellular level even without direct impact on morphological features.

It has been controversially discussed whether there are associations between SRGAP3 gene defects and mental retardation (Endris et al. 2002; Shuib et al. 2009) or not (Hamdan et al. 2009). In a mouse model of metal retardation (Fmr1 knockout mice), spatial learning deficits and memory impairments have been observed, including deficits in the Morris water maze (Baker et al. 2010). Concerning behavior and learning, the SrGAP3-deficient mice did not display alterations in tasks related to hippocampus-associated learning, as, e.g., in the Morris water maze task. This is comparable to the results obtained in another study (Waltereit et al. 2012). Thus, the deficits seen in conditional SrGAP3 knockout mice with respect to, e.g., the Morris water maze (Carlson et al. 2011) could not be seen in the SrGAP3-deficient mice.

The hippocampal formation of SrGAP3$^{-/-}$ mice shows some morphological alterations, including changes in the volume that are due to increased mean thicknesses of the molecular layer of the DG and the *stratum oriens*. Since the non-maternal nest building performance has been shown to be sensitive to hippocampus changes (Jirkof 2014), we analyzed nest building behavior in these mice, but we were unable to detect significant changes in this behavior.

It has been shown that social behavior is impaired in SrGAP3$^{-/-}$ mice (Waltereit et al. 2012). Alteration in social behavior may be linked to schizophrenia, but is also evident in autism spectrum disorders (Banerjee et al. 2014). Some of the mouse models representing syndromic forms of autism

spectrum disorder include mice modeling fragile X syndrome (Banerjee et al. 2014). The most well-known genetic variations that are related to autism spectrum disorder are mutations in Shank3 (Moessner et al. 2007). Shank3-mutant mice display altered behavior and, among others, they show a remarkable failure in solving the marble burying task (Kouser et al. 2013). Moreover, autism has been associated with the V1a receptor gene and V1aR KO mice also display reduced marble burying activity (Egashira et al. 2007). Since SrGAP3-deficient mice also failed to solve the marble burying task, mutation in SrGAP3 might contribute to alterations related to autism spectrum disorder. Along this line, macrocephaly with differential white matter increase is often observed in autism (Williams et al. 2008), and SrGAP3-deficient mice have been reported to display increases in white matter tracts (Waltereit et al. 2012). Moreover, we could show here that SRGAP3-deficient mice display increased thicknesses of the molecular layer of the DG and *stratum oriens* of the hippocampal area CA1. In this context, it should be mentioned that autistic symptoms in children have been linked with hydrocephalus and mental retardation (Fernell et al. 1991).

In humans, distal chromosome 3p deletions (3p-syndrome) are associated with various developmental defects, leading to phenotypes including congenital heart defect, autistic behavior and mental retardation (Harvard et al. 2005; Lauritsen et al. 2006). Specifically, it has been shown that 3p25.3-p26.1 deletion leads to these mentioned phenotypes (Gunnarsson and Foyn Bruun 2010). Such a deletion interrupts several genes in humans, including SrGAP3 (Endris et al. 2002). The term neurodevelopmental disorder refers to disorders including schizophrenia, autism spectrum disorders, epilepsy and mental retardation (Mitchell 2011). Several genes with overlapping functions are known to be causative for intellectual disability, autism and schizophrenia, supporting the existence of shared biologic pathways in these neurodevelopmental disorders (Guilmatre et al. 2009). Among others, SrGAP3 seems to play a multiple role in these neurodevelopmental disorders. SrGAP3-deficient mice have been shown to display a schizophrenia-related intermediate phenotype (Waltereit et al. 2012), and most of them develop a hydrocephalus that might be a consequence of a ciliopathy (Koschützke et al. 2015). Thus, SRGAP3 may represent a gene with a pathological role in several neurodevelopmental disorders.

Acknowledgments We wish to thank Mrs Hanisch, Mr Hadlich and Christian Sperling for excellent technical assistance. We are also grateful to Robert Weissmann for bioinformatic support and thank Dr. Lars R. Jensen for aid with biomolecular analyses. The study was supported by a grant from the "Forschungsverbund Neurowissenschaften" Greifswald and financial aid for the NGS platform used was received from the European Union (EFRE).

References

Bacon C, Endris V, Rappold GA (2013) The cellular function of srGAP3 and its role in neuronal morphogenesis. Mech Dev 130:391–395

Bahi A, Dreyer JL (2012) Hippocampus-specific deletion of tissue plasminogen activator "tPA" in adult mice impairs depression- and anxiety-like behaviors. Eur Neuropsychopharmacol 22:672–682

Baker KB, Wray SP, Ritter R, Mason S, Lanthorn TH, Savelieva KV (2010) Male and female Fmr1 knockout mice on C57 albino background exhibit spatial learning and memory impairments. Genes Brain Behav 9:562–574

Banerjee S, Riordan M, Bhat MA (2014) Genetic aspects of autism spectrum disorders: insights from animal models. Front Cell Neurosci 8: 58

Carlson BR, Lloyd KE, Kruszewski A, Kim IH, Rodriguiz RM, Heindel C, Faytell M, Dudek SM, Wetsel WC, Soderling SH (2011) WRP/srGAP3 facilitates the initiation of spine development by an inverse F-BAR domain, and its loss impairs long-term memory. J Neurosci 31:2447–2460

Couillard-Despres S, Winner B, Schaubeck S, Aigner R, Vroemen M, Weidner N, Bogdahn U, Winkler J, Kuhn HG, Aigner L (2005) Doublecortin expression levels in adult brain reflect neurogenesis. Eur J Neurosci 21:1–14

Deacon RM (2006a) Assessing nest building in mice. Nat Protoc 1:1117–1119

Deacon RM (2006b) Digging and marble burying in mice: simple methods for in vivo identification of biological impacts. Nat Protoc 1:122–124

Dokter M, von Bohlen und Halbach O (2012) Neurogenesis within the adult hippocampus under physiological conditions and in depression. Neural Regen Res 7:8

Egashira N, Tanoue A, Matsuda T, Koushi E, Harada S, Takano Y, Tsujimoto G, Mishima K, Iwasaki K, Fujiwara M (2007) Impaired social interaction and reduced anxiety-related behavior in vasopressin V1a receptor knockout mice. Behav Brain Res 178:123–127

Endris V, Wogatzky B, Leimer U, Bartsch D, Zatyka M, Latif F, Maher ER, Tariverdian G, Kirsch S, Karch D, Rappold GA (2002) The novel Rho-GTPase activating gene MEGAP/ srGAP3 has a putative role in severe mental retardation. Proc Natl Acad Sci U S A 99: 11754–11759

Fernell E, Gillberg C, von Wendt L (1991) Autistic symptoms in children with infantile hydrocephalus. Acta Paediatr Scand 80:451–457

Guilmatre A, Dubourg C, Mosca AL, Legallic S, Goldenberg A, Drouin-Garraud V, Layet V, Rosier A, Briault S, Bonnet-Brilhault F, Laumonnier F, Odent S, Le Vacon G, Joly-Helas G, David V, Bendavid C, Pinoit JM, Henry C, Impallomeni C, Germano E, Tortorella G, Di Rosa G, Barthelemy C, Andres C, Faivre L, Frebourg T, Saugier Veber P, Campion D (2009) Recurrent rearrangements in synaptic and neurodevelopmental genes and shared biologic pathways in schizophrenia, autism, and mental retardation. Arch Gen Psychiatry 66:947–956

Gunnarsson C, Foyn Bruun C (2010) Molecular characterization and clinical features of a patient with an interstitial deletion of 3p25.3-p26.1. Am J Med Genet A 152A:3110–3114

Guo W, Allan AM, Zong R, Zhang L, Johnson EB, Schaller EG, Murthy AC, Goggin SL, Eisch AJ, Oostra BA, Nelson DL, Jin P, Zhao X (2011) Ablation of Fmrp in adult neural stem cells disrupts hippocampus-dependent learning. Nat Med 17:559–565

Hamdan FF, Gauthier J, Pellerin S, Dobrzeniecka S, Marineau C, Fombonne E, Mottron L, Lafreniere RG, Drapeau P, Lacaille JC, Rouleau GA, Michaud JL (2009) No association between SRGAP3/MEGAP haploinsufficiency and mental retardation. Arch Neurol 66:675–676

Harvard C, Malenfant P, Koochek M, Creighton S, Mickelson EC, Holden JJ, Lewis ME, Rajcan-Separovic E (2005) A variant Cri

du Chat phenotype and autism spectrum disorder in a subject with de novo cryptic microdeletions involving 5p15.2 and 3p24.3-25 detected using whole genomic array CGH. Clin Genet 67:341–351

Jirkof P (2014) Burrowing and nest building behavior as indicators of well-being in mice. J Neurosci Methods 234:139–146

Kempermann G (2012) New neurons for 'survival of the fittest'. Nat Rev Neurosci 13:727–736

Kim IH, Carlson BR, Heindel CC, Kim H, Soderling SH (2012) Disruption of wave-associated Rac GTPase-activating protein (Wrp) leads to abnormal adult neural progenitor migration associated with hydrocephalus. J Biol Chem 287:39263–39274

Koschützke L, Bertram J, Hartmann B, Bartsch D, Lotze M, von Bohlen und Halbach O (2015) SrGAP3 knockout mice display enlarged lateral ventricles and specific cilia disturbances of ependymal cells in the third ventricle. Cell Tissue Res 361:645–650

Kouser M, Speed HE, Dewey CM, Reimers JM, Widman AJ, Gupta N, Liu S, Jaramillo TC, Bangash M, Xiao B, Worley PF, Powell CM (2013) Loss of predominant Shank3 isoforms results in hippocampus-dependent impairments in behavior and synaptic transmission. J Neurosci 33:18448–18468

Lauritsen MB, Als TD, Dahl HA, Flint TJ, Wang AG, Vang M, Kruse TA, Ewald H, Mors O (2006) A genome-wide search for alleles and haplotypes associated with autism and related pervasive developmental disorders on the Faroe Islands. Mol Psychiatry 11:37–46

Li X, Morrow D, Witkin JM (2006) Decreases in nestlet shredding of mice by serotonin uptake inhibitors: comparison with marble burying. Life Sci 78:1933–1939

Lu H, Jiao Q, Wang YY, Yang ZQ, Feng MJ, Wang L, Chen XL, Jin WL, Liu Y (2013) The mental retardation associated protein srGAP3 regulates survival, proliferation and differentiation of rat embryonic neural stem/progenitor cells. Stem Cells Dev 22:1709–1716

Marlatt MW, Potter MC, Lucassen PJ, van Praag H (2012) Running throughout middle-age improves memory function, hippocampal neurogenesis, and BDNF levels in female C57BL/6J mice. Dev Neurobiol 72:943–952

Mitchell KJ (2011) The genetics of neurodevelopmental disease. Curr Opin Neurobiol 21:197–203

Moessner R, Marshall CR, Sutcliffe JS, Skaug J, Pinto D, Vincent J, Zwaigenbaum L, Fernandez B, Roberts W, Szatmari P, Scherer SW (2007) Contribution of SHANK3 mutations to autism spectrum disorder. Am J Hum Genet 81:1289–1297

Powell CM, Schoch S, Monteggia L, Barrot M, Matos MF, Feldmann N, Sudhof TC, Nestler EJ (2004) The presynaptic active zone protein RIM1alpha is critical for normal learning and memory. Neuron 42: 143–153

Puma C, Bizot JC (1998) Intraseptal infusions of a low dose of AP5, a NMDA receptor antagonist, improves memory in an object recognition task in rats. Neurosci Lett 248:183–186

Sharma S, Rakoczy S, Brown-Borg H (2010) Assessment of spatial memory in mice. Life Sci 87:521–536

Sholl DA (1953) Dendritic organization in the neurons of the visual and motor cortices of the cat. J Anat 87:387–406

Shuib S, McMullan D, Rattenberry E, Barber RM, Rahman F, Zatyka M, Chapman C, Macdonald F, Latif F, Davison V, Maher ER (2009) Microarray based analysis of 3p25-p26 deletions (3p- syndrome). Am J Med Genet A 149A:2099–2105

Vogt MA, Chourbaji S, Brandwein C, Dormann C, Sprengel R, Gass P (2008) Suitability of tamoxifen-induced mutagenesis for behavioral phenotyping. Exp Neurol 211:25–33

von Bohlen und Halbach O (2011) Immunohistological markers for proliferative events, gliogenesis, and neurogenesis within the adult hippocampus. Cell Tissue Res 345:1–19

von Bohlen und Halbach O, Zacher C, Gass P, Unsicker K (2006) Age-related alterations in hippocampal spines and deficiencies in spatial memory in mice. J Neurosci Res 83:525–531

von Bohlen und Halbach O, Lotze M, Pfannmöller JP (2014) Postmortem magnetic resonance microscopy (MRM) of the murine brain at 7 Tesla results in a gain of resolution as compared to in vivo MRM. Front Neuroanat 8:1–7

Waltereit R, Kautt S, Bartsch D (2008) Expression of MEGAP mRNA during embryonic development. Gene Expr Patterns 8:307–310

Waltereit R, Leimer U, von Bohlen und Halbach O, Panke J, Holter SM, Garrett L, Wittig K, Schneider M, Schmitt C, Calzada-Wack J, Neff F, Becker L, Prehn C, Kutscherjawy S, Endris V, Bacon C, Fuchs H, Gailus-Durner V, Berger S, Schonig K, Adamski J, Klopstock T, Esposito I, Wurst W, de Angelis MH, Rappold G, Wieland T, Bartsch D (2012) Srgap3-/- mice present a neurodevelopmental disorder with schizophrenia-related intermediate phenotypes. FASEB J 26:4418–4428

Williams CA, Dagli A, Battaglia A (2008) Genetic disorders associated with macrocephaly. Am J Med Genet A 146A:2023–2037